

Registration Simulations and Sampling Strategies for Large Field Lithography

Gary E. Flores and Warren W. Flack

Ultratech Stepper, Inc., San Jose, CA 95134

Joseph C. Pellegrini

New Visions Systems, Watertown, MA 02172

Mark Merrill

KLA Instruments Corporation, San Jose, CA 95161

Author Biographies

Gary E. Flores is a senior applications engineer at Ultratech Stepper where he is responsible for application support and development of lithography stepper processes. He received his BS degree in chemical engineering from the University of California at Berkeley in 1983 and MS degree from the University of California at Santa Barbara in 1985. Prior to joining Ultratech Stepper, he was employed with KTI Chemicals, Inc. as a senior technical development engineer, where he worked on the development of lithographic materials and processes. From 1985 through 1990 he worked at TRW's Microelectronics Center as a senior process engineer, with responsibilities in optical lithography, dry etching and wet etching.

Warren W. Flack is the Asian applications manager for Ultratech Stepper based out of Tokyo, Japan. He is responsible for customer applications support for thin film head and silicon semiconductor applications. Before joining Ultratech Stepper in 1992, he was senior section head for pattern transfer at TRW's Microelectronic Center. There, he was responsible for optical lithography, electron-beam lithography and dry etching for advanced silicon technologies. He received his BS and MS degrees in Chemical Engineering from the Georgia Institute of Technology in 1978 and 1979 and his PhD in Chemical Engineering from the University of California at Berkeley in 1983.

Joseph C. Pellegrini received his BS and MS degrees studying microprocessor control systems in the Aeronautics and Astronautics Department at the Massachusetts Institute of Technology. He is the president of New Vision Systems, Inc. (NVS) of Watertown, Massachusetts, a company that develops industrial control and analysis systems and is the driving force behind the MONO-LITH Analysis Packages. In addition to his duties at NVS, Mr. Pellegrini has also lectured at MIT on topics including real-time computer systems and software engineering.

Abstract

Overlay registration models are well developed for environments using similar types of lithography equipment. In this scenario, a 1:1 field size matching is the standard registration requirement. However, there is now significant interest in mix-and-match lithography utilizing steppers with extremely large field

sizes (large field steppers) to increase wafer throughput on less critical process levels, and use advanced reduction steppers with a smaller field (standard field steppers) for the critical levels. Large field steppers typically have two to four times the field size of advanced 5x reduction steppers (2:1 to 4:1), and thus, application of traditional 1:1 registration analysis techniques will not produce optimal results. In order to properly characterize and optimize such an n:1 matching scheme, one must consider the types of registration errors present and their sources.

For the case of 2:1 field matching, there are several unique effects of registration error sources resulting from the field placement geometry. A series of matching errors is illustrated using overlay error vector plots generated from a lithography simulator for 2:1 field matching. This provides valuable insight into understanding how various combinations of grid and intrafield errors are manifested for 2:1 field matching. For example, lens magnification on either the large field or standard field stepper can manifest itself as an apparent combination of scale errors from both steppers. It is also possible to have intrafield bifurcation of overlay errors or mean offset differences between alternating pairs of standard stepper fields within the large stepper fields. It has been observed that intrafield rotation can induce an apparent grid rotation. These effects illustrate the necessity of using proper models for characterizing and optimizing overlay errors in the 2:1 matching domain.

Overlay sampling schemes for interfield and intrafield errors are well developed for the case of 1:1 registration. However, the unique registration errors resulting from the 2:1 geometry suggests that sampling schemes should be re-evaluated for large field lithography. A variety of sample plans based on 2:1 registration are investigated. A large data set sample plan is outlined and the various sample plans are simulated using subsets of this data. Analysis of 2:1 simulated overlay results shows that it is necessary to revise both production and maintenance monitoring sampling strategies to take into account field matching asymmetries.

1.0 Introduction

Over the last decade, the international competition in integrated circuit fabrication has been based on both technological and economic factors. However, fabrication costs are now becoming the single dominant issue as the price of new high-volume production facilities approaches the billion dollar level [1]. Since lithography equipment represents a large fraction of this investment cost, it is also an excellent area in which to pursue cost savings [1]. One technique that has been extremely successful in containing lithographic costs is mix-and-match lithography.

Mix-and-match lithography has been used to bridge different systems to derive the maximum benefits of each. Mix-and-match was first widely used during the transition from scanners and steppers. This approach allowed fabrication facilities to take advantage of their installed base of scanners while achieving the resolution and overlay of the steppers for critical levels [2]. More recently, mix-and-match lithography has been used between steppers and extremely expensive, high-performance lithography

equipment such as direct write-on wafer e-beam or x-ray systems [3]. This approach offered significant fabrication cost savings while maintaining technological advantages.

In general, a less costly and higher throughput lithography tool is used for the non-critical levels, while the higher resolution and more expensive lithography tool is only used on critical levels. This approach provides dramatic cost-of-ownership advantages over using the more expensive critical level lithography tool on all levels [1,4]. Higher throughput for non-critical levels can be achieved by lithography systems with a large lens field size that reduces the number of exposure steps required for each wafer. However, this larger field size must be an integer multiple (n) of the field size of the standard field lithography tool to reduce the number of exposure steps. The $n:1$ ratio varies between two and four for currently available large field lithography systems. For example, the Ultratech 2244i 1x stepper has a rectangular field size of 22 x 44 mm, which is twice the 22 x 22 mm square field size of current 5x reduction steppers from ASM, Canon and Nikon [5]. For each stepped position, the Ultratech (large field) stepper simultaneously patterns two horizontally spaced 5x reduction (standard field) stepper fields as shown in figure 1. Here ΔX and ΔY represent the stage motion in the X and Y directions respectively.

To obtain maximum performance when using multiple lithographic systems, each system must be calibrated or matched to the others [6]. Extensive analysis and modeling of overlay errors has been developed for the matching of similar systems. These overlay errors can be divided into intrafield and interfield systematic sources. The intrafield sources (dX and dY) model the overlay error sources within one field [7,8,9]:

$$dX(x,y) = T_{ix} + M_x x - \Theta_i y + \Psi_x xy + \Psi_y x^2 + D_3 x(x^2+y^2) + D_5 x(x^2+y^2)^2 \quad (1)$$

$$dY(x,y) = T_{iy} + M_y y + \Theta_i x + \Psi_y xy + \Psi_x y^2 + D_3 y(x^2+y^2) + D_5 y(x^2+y^2)^2 \quad (2)$$

where x and y are the coordinate location relative to the center of the field. For equations (1) and (2), the linear terms include die shift in x (T_{ix}) and y (T_{iy}), magnification in x (M_x) and y (M_y) and rotation (Θ_i). The nonlinear terms include trapezoid in x (Ψ_x) and y (Ψ_y) third order (D_3) and fifth order (D_5). The interfield or grid sources (E_x and E_y) model the system stage motion errors across the wafer [8,9]:

$$E_x(X,Y) = T_{gx} + S_x X - \Theta_g Y - \Phi Y \quad (3)$$

$$E_y(X,Y) = T_{gy} + S_y Y + \Theta_g X \quad (4)$$

where X and Y are the coordinate locations on the wafer. The interfield sources include translation error in X (T_{gx}) and Y (T_{gy}), wafer scaling magnification in X (S_x) and Y (S_y), wafer rotation (Θ_g), and wafer orthogonality (Φ). The orthogonality term defined in equation (3) is actually a skew which contains both pure rotation and orthogonality components. However, for this study it will be referred to as orthogonality.

These intrafield and interfield models assume identical field sizes, which implies 1:1 field matching. However, mix-and-match lithography frequently requires $n:1$ field matching for high throughput. This means that the standard size fields can not be concentrically positioned on the large field stepper. Non-

concentric field matching has been studied for the case of two different field size reduction steppers [10]. This arrangement typically results in 4:1 field matching which can create large overlay errors at various points within the field, not just at extreme corners of the large field. The conclusions from this analysis were that the ideal lens for mix-and-match lithography should have as little distortion as possible relative to an absolute grid. Therefore, it is not appropriate to simply match lenses relative to the distortions built into previous generation systems.

A grid overlay model for the specific case of 2:1 matching has been developed [11]. It was compared with two classical grid approaches, a 1:1 model with the standard field stepper as the reference level and a 1:1 model with the large field as the reference level. The 2:1 model grid coefficients were calculated using a beta version of Mono-Lith[®] [9], while model coefficients for the 1:1 models were determined from KLASS III[®] software [12]. Experimental data for the grid model verification was obtained using a Canon 2500i2 as the standard field stepper and a Ultratech 2244i as the large field stepper. Comparisons of the three grid models illustrate the superior performance of the 2:1 grid overlay model. Both 1:1 models show comparable residuals while the 2:1 model shows a 29% residual improvement [11]. An overlay model that includes both grid and intrafield effects for n:1 matching is very complex to develop. However, a simulator can be created which allows the visualization of overlay errors, which result from the n:1 geometry. In this manner it is possible to determine the importance of using geometrically correct models to obtain optimal performance for mix-and-match lithography.

The validity of existing 1:1 overlay sampling schemes for large field lithography has not been established. The simulation results in this study show that 2:1 intrafield and interfield overlay errors are not intuitive in nature. This suggests that existing sampling schemes need to be modified to correctly model distortions. Lens distortion characterization for 1:1 registration typically requires at least 17 sites per field to determine the higher order interfield components for system maintenance qualification [6]. Typically, five fields per wafer and four sites per field are used for process monitoring in a production environment [12]. The importance of symmetry and spacial coverage in the selection of these sample sites has been established experimentally [13]. When using n:1 matching, this classical approach can no longer be assumed to be optimal. Distortions are asymmetric and can often be the largest in the center of the field or near a critical geometry of the device being manufactured. Process control can only be done using an effective overlay sampling plan that is able to estimate the overlay variance across the wafer and in the lens field. Again, an overlay simulator can be used to show the effectiveness of these sampling schemes for n:1 geometries.

2.0 Simulation Modeling

Simulation of grid and intrafield errors for n:1 field matching provides an illustrative technique to understand the resulting mix-and-match overlay error. A simulator designed specifically for 2:1 field matching was developed for this project using Mono-lith[®] software. The 2:1 simulator allows generation of grid and intrafield errors for standard and large field steppers using equations (1) through (4).

The simulated results are arranged in a 4 by 4 wafer matrix of standard type fields, each with a field size of 22 x 22 mm. Alternatively, this can be viewed as a large field matrix of 2 columns and 4 rows with a field size of 44 x 22 mm. The intrafield grid contains 9 locations in a 3 by 3 array for the standard field stepper, where each grid location is spaced 6.5 mm. For the large field stepper the same 6.5 mm spacing was used for a total of 18 grid locations in an array of 3 rows and 6 columns. This format provides for a total of 144 grid locations for visual representation.

To understand the simulation overlay errors for 2:1 field matching, it is informative to examine the error sources for the standard and large field steppers independently, and then demonstrate the net effect of both for mix-and-match. Because of the 2:1 matching geometry in the x axis, comparable error sources from both the large field and standard field steppers will not necessarily provide zero residual error. For the case of 4:1 matching, this effect would be observed in both the x and y axis. The four sample scenarios selected for examination are wafer scale magnification in X , intrafield magnification, wafer grid orthogonality and intrafield rotation.

2.1 Wafer Scaling Magnification in X Simulation

Figure 2 illustrates the simulation of wafer scaling magnification in X (S_x) with errors of +10 ppm (parts per million) for the standard field stepper and -5 ppm for the large field stepper. The figure shows the standard field errors, the large field errors and the combination errors in sections a, b and c respectively. The +10 ppm X wafer scale for the standard field results in a stepped increase in overlay error in the X direction for each field from the center. In comparison, the -5 ppm large field scale error results in an incremental error in the opposite direction from the standard field scale error in the X direction, but the errors remain consistent over the large field geometry. The combination of the X scale errors for mix-and-match results in a net residual scale error. It is interesting that the combined error is zero for the center two columns of the standard field, while the outer two rows have a net residual error. Clearly, this type of net error would be impossible to explain using a 1:1 field model analysis.

2.2 Intrafield Magnification in x (M_x) and y (M_y) Simulation

This example considers equal and opposite intrafield magnification errors on both type steppers. Figure 3 shows the intrafield magnification in x (M_x) and y (M_y) for the standard field and large field steppers of +10 ppm and -10 ppm respectively. For the standard field stepper, the intrafield magnification of +10 ppm results in maximum error vector of 220 nanometers (nm) at the edge of the field (10 ppm times the field size of 22 mm) in both the x and y directions. For the large field stepper an intrafield magnification -10 ppm results in a maximum error vector of 220 ppm in the y dimension at the edge of the field, but in the opposite direction. However, the error vector is 440 nm in the x direction since the large field dimension is twice that of the standard field. Therefore, when both the standard and large field magnification errors are combined, the net result is a residual x mean offset difference between alternating standard field columns. This net residual can be viewed within the large field domain as a symmetric x mean offset across the left and right portions of the field that are equal but of opposite magnitude.

2.3 Wafer Grid Orthogonality Simulation

Wafer grid orthogonality (Φ) is another interesting example where it is useful to consider equal and opposite errors on the standard and large field steppers. Here grid orthogonality errors of -10 ppm and +10 ppm for the standard field and large field steppers are shown in sections a and b of Figure 4. Since wafer grid orthogonality occurs as a step change with wafer field location, all vector errors are oriented in the same x and y direction for a given large or standard field position. In addition, the error magnitude is dependent on grid location since orthogonality is a function of the wafer grid. It is interesting to observe the impact of combining the standard and large field grid components. In this case two horizontal standard fields containing different error vector magnitudes are combined with a single large field containing constant error vectors over the entire field. The net result is a mean y offset error across the large field. These errors occur in alternating standard field columns with equal and opposite errors. Here the x component of the individual orthogonality errors combine for a net zero offset. What is also unique is that the grid based nature of the orthogonality error no longer exists. As in the previous cases, such results could not be explained using a classical 1:1 field model.

2.4 Intrafield Rotation Simulation

Intrafield rotation (Θ_i) due to reticle placement errors also shows a similar behavior to that of the wafer grid orthogonality. In this example intrafield rotation errors of -10 ppm and +10 ppm for the standard field and large field steppers are shown in the a and b sections of Figure 5. In both cases, the intrafield rotation point is at the x and y center of each stepper field. Unlike the previous orthogonality example, intrafield rotation does not depend on field placement. The combined effect of these errors is shown in section c of Figure 5. The residual error is manifested as a y mean offset across the large field stepper domain. As in the previous example, these errors occur in alternating standard field columns with equal and opposite magnitude.

3.0 Sampling Schemes and Modeling

3.1 Sampling Strategies

Sampling strategies for 1:1 registration are well established in the literature. For interfield or grid based sources, a common strategy utilized is five fields per wafer arranged in a cross on the wafer [12, 13]. An example of this field layout is shown in Figure 6 for both large field and standard field steppers. Such a layout benefits from symmetry which is crucial for regression analysis to calculate interfield sources. In terms of statistical significance in the regression analysis, five field sites provide four additional degrees of freedom for error analysis. A minimum of five locations per field are preferred for intrafield sampling in 1:1 registration [12]. Typically the four corners of the lens field and the center of the field are utilized. However, in most manufacturing environments, the center of the field is unavailable since it is reserved for

product die. The five intrafield locations are illustrated in scheme 1 of Figure 7 for two adjacent standard fields.

The simulation modeling described in section 2.0 has shown that 2:1 registration effects are not necessarily intuitive nor can they be described using 1:1 registration analysis. This suggests that it is important to use appropriate sampling schemes to provide adequate characterization for 2:1 field matching. Therefore, it was decided to evaluate the impact of a variety of different sampling schemes on 2:1 registration modeling.

The eight-inch wafer layout in Figure 6 was used for all of the sampling schemes. The wafer consists of a matrix of 7 rows and 6 columns of a standard size field (22 x 22 mm). This wafer can also be viewed as a matrix of 7 rows and 3 columns for a large size field (44 x 22 mm). This represents the same type of 2:1 field matching as presented in the simulation modeling section. Figure 6 shows the five shaded large fields in a classic cross pattern that were selected for sampling. The intrafield grid array was constructed with 3 by 3 sites per standard field using a spacing of 6.5 mm. For the large field stepper the same 6.5 mm spacing was used for a total of 18 sites in an array of 3 rows and 6 columns. This format provides for a total of 378 grid locations per wafer.

The same four scenarios presented in the simulation modeling section were evaluated using six different sampling schemes. The systematic grid and intrafield error sources were simulated as in the simulation modeling section. However, in addition a random error component was included in the simulated data set. This noise term is critical to account for the random error components due to lithography and metrology errors. For this analysis, the random errors were estimated at 80 nm from the lithography tool, 5 nm for metrology repeatability and 5 nm for tool induced shift (TIS). A root mean squared addition of these random error terms provided a three sigma of 80.3 nm.

3.2 Intrafield Sampling Schemes

Figure 7 depicts the six unique intrafield sampling schemes that were examined for each of the four simulation scenarios. Scheme 1 is a logical extension of the basic five intrafield locations per field that are recommended for 1:1 field matching. In this case, the five sites are sampled in each standard field which corresponds to ten locations per large field. Scheme 2 is more applicable for a manufacturing environment since it eliminates the center location of each standard field. Scheme 3 simply ignores the 2:1 matching issue and samples the four corners of the large field. Since this layout samples at the extreme locations of the large field, it should indicate effects due to apparent die rotation or field magnification. Scheme 4 provides samples at the top left and right locations of each standard field for a total of 4 locations per large field. Scheme 5 is the minimum sample size with one site per standard field required to show rotation effects. Note that these first five schemes all show symmetry in the large field domain. An asymmetric scheme would tend to bias the relative errors of adjacent standard fields and produce potentially misleading results for 2:1 field matching. Scheme 6 containing three sites was included to explore the impact of asymmetric sampling.

3.3 Wafer Scaling Magnification in X Sampling

Figure 8 illustrates the modeled grid coefficients due to wafer scaling magnification in X (S_x) with simulated errors of +10 ppm for the standard field stepper and - 5 ppm for the large field stepper. The modeled grid coefficients are graphed for the six sampling schemes. The top graph shows the X and Y scale terms while the bottom graph shows rotation and orthogonality components. Sampling schemes 1 through 5 all demonstrate excellent performance for determination of the simulated X wafer scaling. However the asymmetric scheme 6 is unable to properly determine the X wafer scaling.

3.4 Intrafield Magnification in x (M_x) and y (M_y) Sampling

Figure 9 illustrates the modeled grid coefficients which result from equal and opposite intrafield magnification errors in x (M_x) and y (M_y). The simulated intrafield magnification errors are +10 ppm for the standard field stepper and - 10 ppm for the large field stepper. As previously shown in Figure 3, this scenario causes an x mean offset between alternating standard fields. Figure 9 shows that schemes 1 through 5 yield equal and opposite X scale errors of +10 ppm and -10 ppm for the large and standard field steppers, although the simulated X scale errors were actually 0 ppm. This effect occurs since the net magnification error due to both steppers are actually correctable by an X scale compensation on each stepper. This is an interesting case where the $n:1$ field geometry allows a grid factor to correct an intrafield error. All six schemes provide essentially no apparent grid orthogonality corrections. However, scheme 5 shows a large rotation offset for both steppers as a result of the minimum sampling of one site for each standard field.

3.5 Wafer Grid Orthogonality Sampling

Figure 10 illustrates the modeled grid coefficients for equal and opposite wafer grid orthogonality errors on both steppers. The simulated wafer grid orthogonality errors are -10 ppm for the standard field stepper and + 10 ppm for the large field stepper. As previously shown in Figure 4, this scenario causes a net y mean offset between alternating standard fields. The modeled grid coefficients are all graphed versus sampling scheme in Figure 10. In this case, it is interesting that the X scale corrections for each stepper are of equal and opposite magnitude for each sampling scheme. Note that as the number of sampling sites is decreased, the magnitude of the scale corrections becomes substantially larger. All six sampling schemes perform well in determining the simulated orthogonality errors.

3.6 Intrafield Rotation Sampling

Figure 11 illustrates the modeled grid coefficients when equal and opposite intrafield rotations errors occur on both steppers. The simulated intrafield errors are -10 ppm for the standard field stepper and + 10 ppm for the large field stepper. The modeled X and Y scale errors for both steppers is relatively small for schemes 1 to 4, while schemes 5 and 6 start to show a departure from zero. However, a common feature is

that all six schemes yield equal and opposite wafer grid rotation errors of + 10 ppm and -10 ppm for the standard field and large field steppers. This effect occurs since the intrafield rotation errors are manifested in a similar manner as the wafer grid rotation in the previous example. This type of intrafield error can be corrected by a wafer grid correction as a result of the n:1 geometry.

3.7 Residual Error Comparison

An effective technique to compare each of the six sampling schemes is a residual error analysis. For this study, the residual error is defined as the overlay error remaining after application of grid and intrafield reticle rotation corrections. Here all the modeled grid corrections for the standard and large field stepper are removed from the entire simulated data set along with the modeled reticle rotation of the large field stepper.

Figure 12 displays the four scenarios with x and y residual standard deviation for each of the six sampling schemes. For the wafer scaling in X , sampling schemes 1 through 3 show comparable results in both x and y , while schemes 4 through 6 yield progressively worse x errors. It is reasonable that the y residual error remains stable for schemes 1 through 5, since the major error source simulated was an X scale error. The large error in scheme 6 is due to the generation of a field reticle rotation from the asymmetric sampling scheme.

The intrafield magnification scenario also shows a strong dependence on the sampling scheme used for corrections with the worst performance occurring for scheme 6. Figure 9 showed that schemes 1 through 5 yielded large but equal and opposite X scale corrections. These provide a compensation for the magnification errors of each stepper.

For the wafer grid orthogonality example, schemes 1 and 2 provide the lowest x and y residual errors. Schemes 3 through 5 show radically different residual errors. Interestingly, scheme 6 performed better than schemes 3 through 5. The main difference between these schemes are the modeled intrafield reticle rotation corrections, which are extremely sensitive to sampling scheme.

In the final case, the residual x and y errors for the example intrafield reticle rotations are also strongly dependent on sampling scheme. Here schemes 1, 2 and 4 provide excellent results, while 3, 5 and 6 show progressively worse results. Note that the y residual in scheme 6 is actually six times worse than schemes 1, 2 and 3.

4.0 Conclusions

With the continued escalating costs of advanced lithography equipment for the semiconductor industry, mix-and-match lithography is becoming widely accepted as a technique to achieve cost savings. However, the lithography inherent to mix-and-match requires n:1 field overlay matching which can not be optimized fully using classic 1:1 models.

A grid and interfield simulator has been developed for 2:1 field matching. Simulations have been explored to understand the unique effects of registration error sources resulting from the 2:1 geometry. For example, lens magnification on either the large field or standard field stepper can manifest itself as apparent combinations of mean scale errors from both steppers. It is also possible to have intrafield errors or mean offset differences between alternating pairs of standard stepper fields and within the large stepper fields due to equal and opposite errors such as orthogonality, intrafield rotation and intrafield magnification.

The unique registration errors for 2:1 matching suggested that sampling schemes should be re-evaluated for large field lithography. Six different sample plans based on 2:1 registration were investigated using the grid and interfield simulator. A strong sensitivity to sampling strategy was observed. The recommended scheme from this study is four corner points per standard field, or 8 points per large field.

The simulation results in this study illustrate the necessity of using proper models and overlay sampling schemes for characterizing and optimizing overlay errors in any n:1 matching domain.

5.0 References

1. J. Maltabes, M. Hakey, A. Levine, "Cost/Benefit Analysis of Mix-and-Match Lithography for Production of Half-Micron Devices", *Optical/Laser Lithography VI Proceedings*, SPIE **1927** (1993).
2. W. Arnold, "Image Placement Differences Between 1:1 projection Aligners and 10:1 Reduction Wafer Steppers", *Optical Microlithography II Proceedings*, SPIE **394** (1983).
3. W. Flack, D. Dameron, G. Maleck and V. Alameda, "Mix-and-Match Lithography in a Manufacturing Environment", *Electron-Beam, X-Ray and Ion Beam Submicrometer Lithographies for Manufacturing II Proceedings*, SPIE **1674** (1992).
4. M. Perkins and J. Stamp, "Intermix Technology: The Key to Optimal Stepper Productivity and Cost Efficiency", *Optical/Laser Microlithography V Proceedings*, SPIE **1674** (1992).
5. G. Flores, W. Flack, L. Dwyer, "Lithographic Performance of a New Generation i-line Optical System: A Comparative Analysis", *Optical/Laser Lithography VI Proceedings*, SPIE **1927** (1993).
6. A. Yost and W. Wu, "Lens Matching and Distortion in a Multi-stepper, Sub-micron Environment", *Integrated Circuit Metrology, Inspection and Process Control III Proceedings*, SPIE **1087** (1989).
7. J. Armitage, "Analysis of Overlay Distortion Patterns", *Integrated Circuit Metrology, Inspection and Process Control II Proceedings*, SPIE **921** (1988).
8. M. van den Brink, C. de Mol and R. George, "Matching Performance for Multiple Wafer Steppers Using an Advanced Metrology Procedure", *Integrated Circuit Metrology, Inspection and Process Control II Proceedings*, SPIE **921** (1988).
9. Mono-Lith[®] Reference Manual, version 2.08, Registration Models and Algorithms.

10. M. Preil, T. Manchester, A. Minvielle, R. Chung, “Minimization of Total Overlay Errors when Matching Non-Concentric Exposure Fields”, *Optical/Laser Microlithography VII Proceedings*, SPIE **2197** (1994).
11. W. Flack, G. Flores, J. Pellegrini and M. Merrill, “An Optimized Registration Model for 2:1 Stepper Field Matching”, *Optical/Laser Microlithography VII Proceedings*, SPIE **2197** (1994).
12. KLASS III[®] Reference Manual, Appendix Models and Algorithms.
13. I. Fink, N. Sullivan, J. Lekas, “Overlay Sample Plan Optimization for the Detection of Higher Order Contributions to Misalignment”, *Integrated Circuit, Metrology, Inspection and Process Control VIII*, SPIE **2196** (1994).

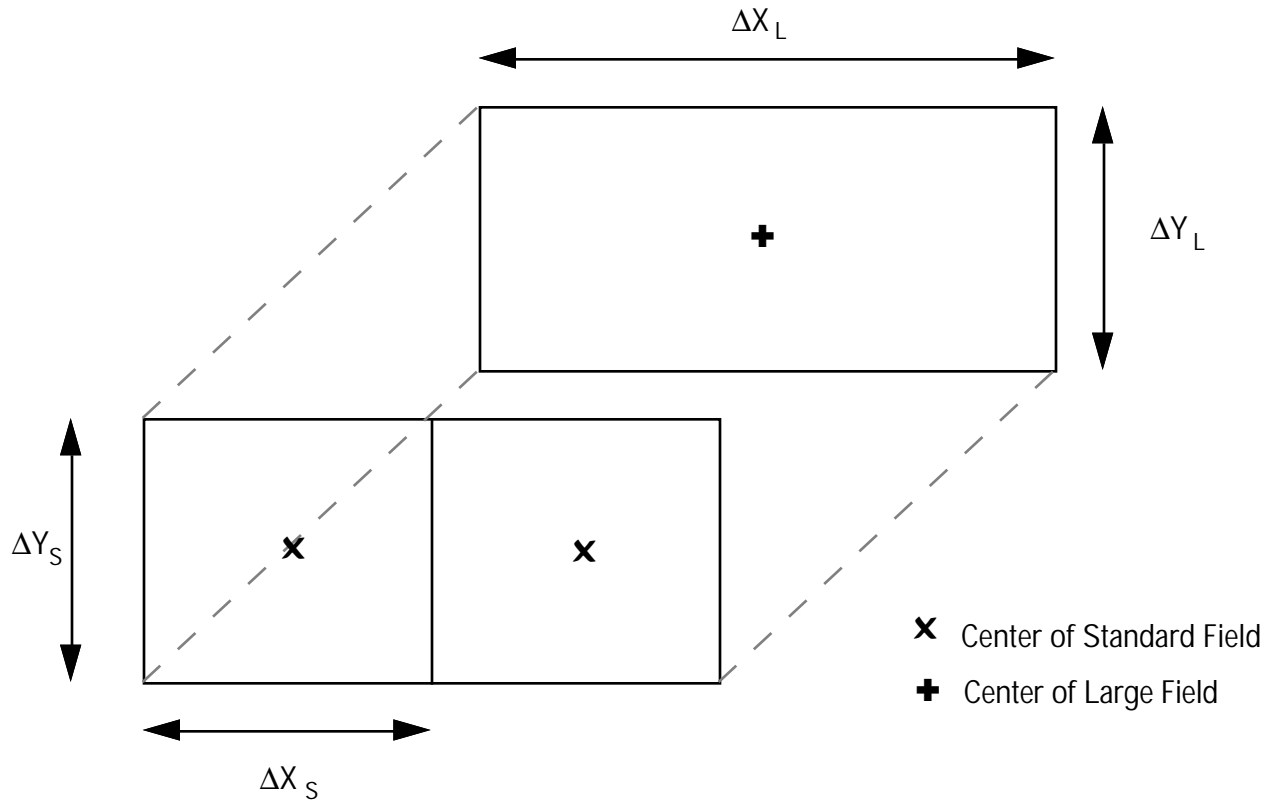
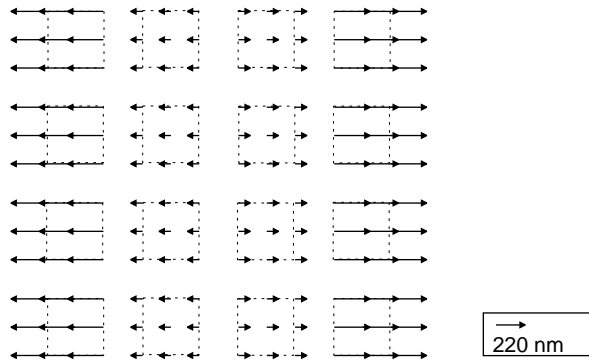
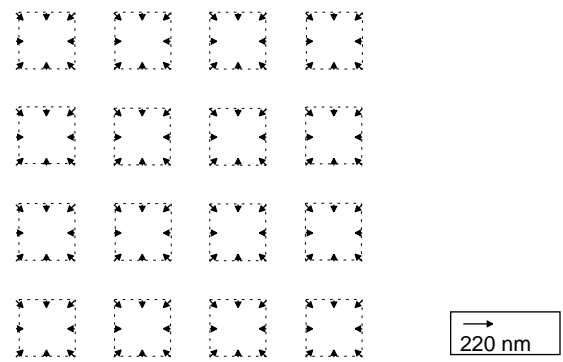


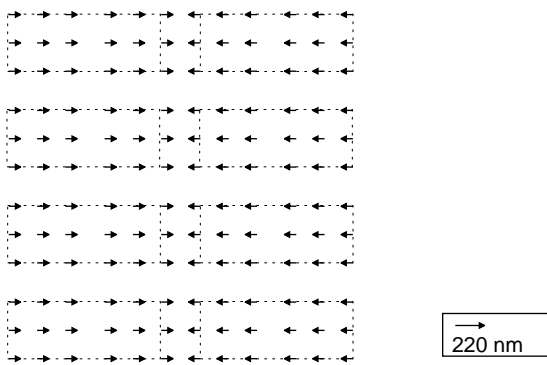
Figure 1: Exploded view of 2:1 field overlay



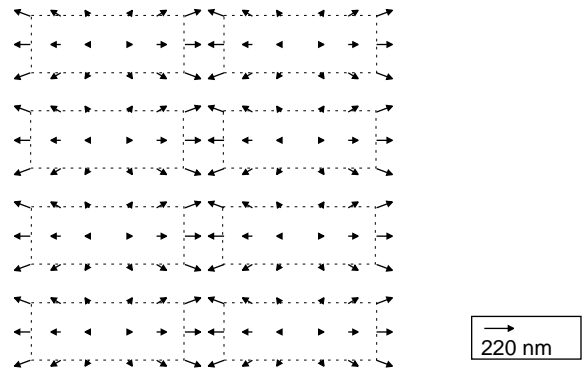
a) Standard Field



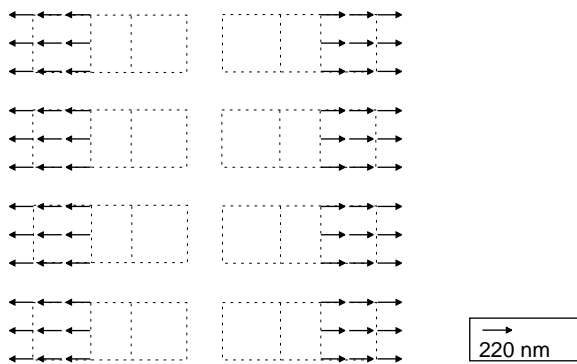
a) Standard Field



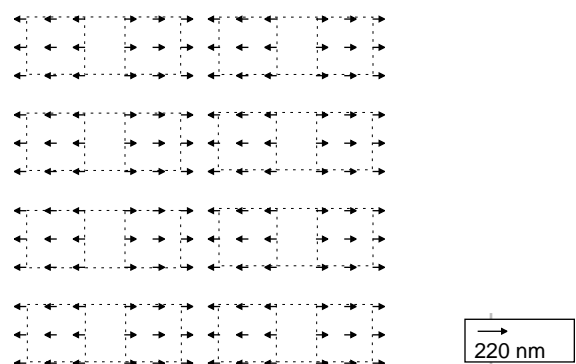
b) Large Field



b) Large Field



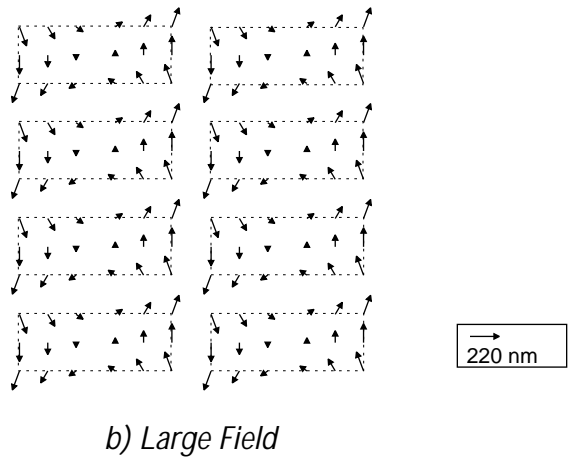
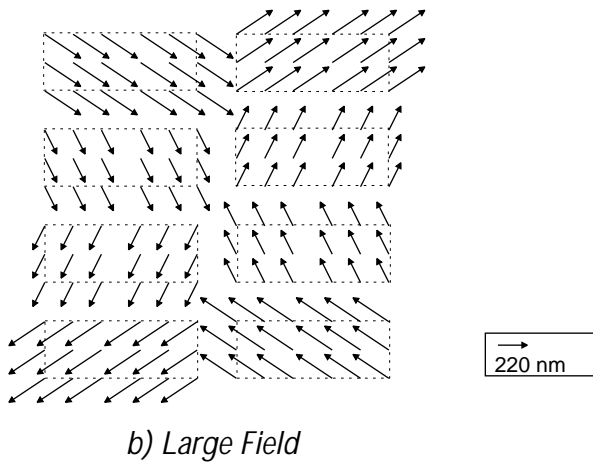
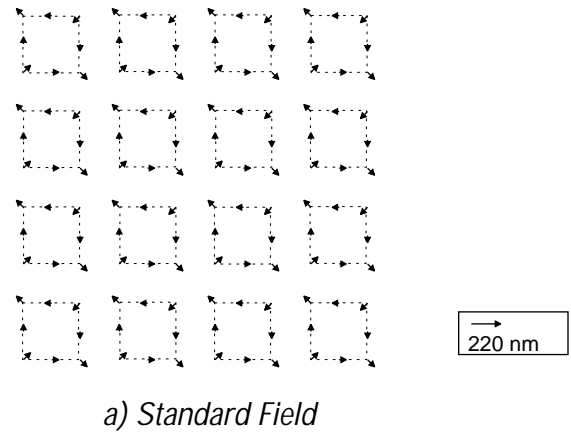
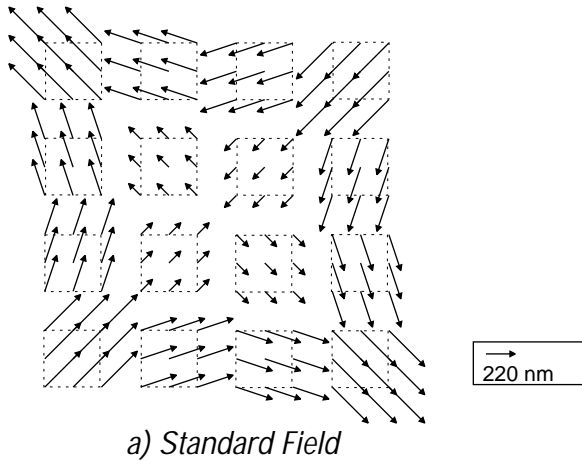
c) Combination

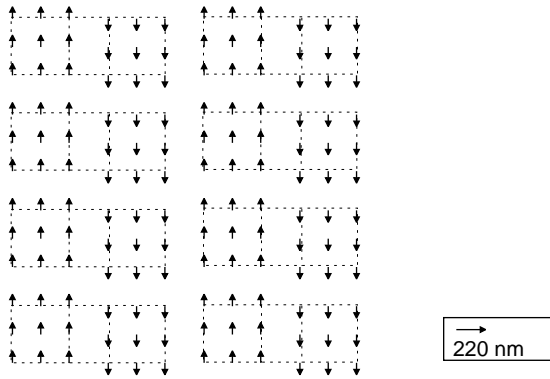


c) Combination

Figure 2: Simulation of X scale errors on the wafer grid. The standard field error is +10ppm and the large field error is -5ppm.

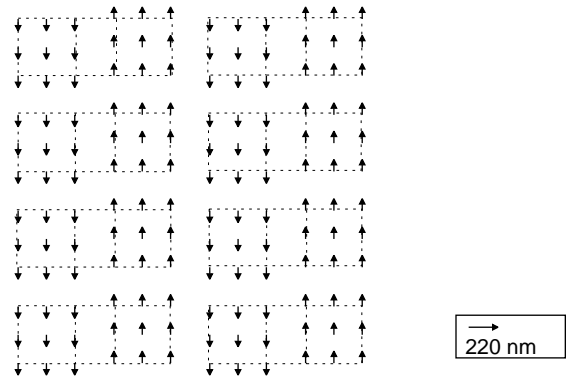
Figure 3: Simulation of intrafield magnification errors. The standard field error is +10ppm and the large field error is -10ppm.





c) Combination

Figure 4: Simulation of orthogonality on the wafer grid. The standard field error is -10ppm and the large field error is +10ppm.



c) Combination

Figure 5: Simulation of intrafield rotation errors. The standard field error is -10ppm and the large field error is +10ppm.

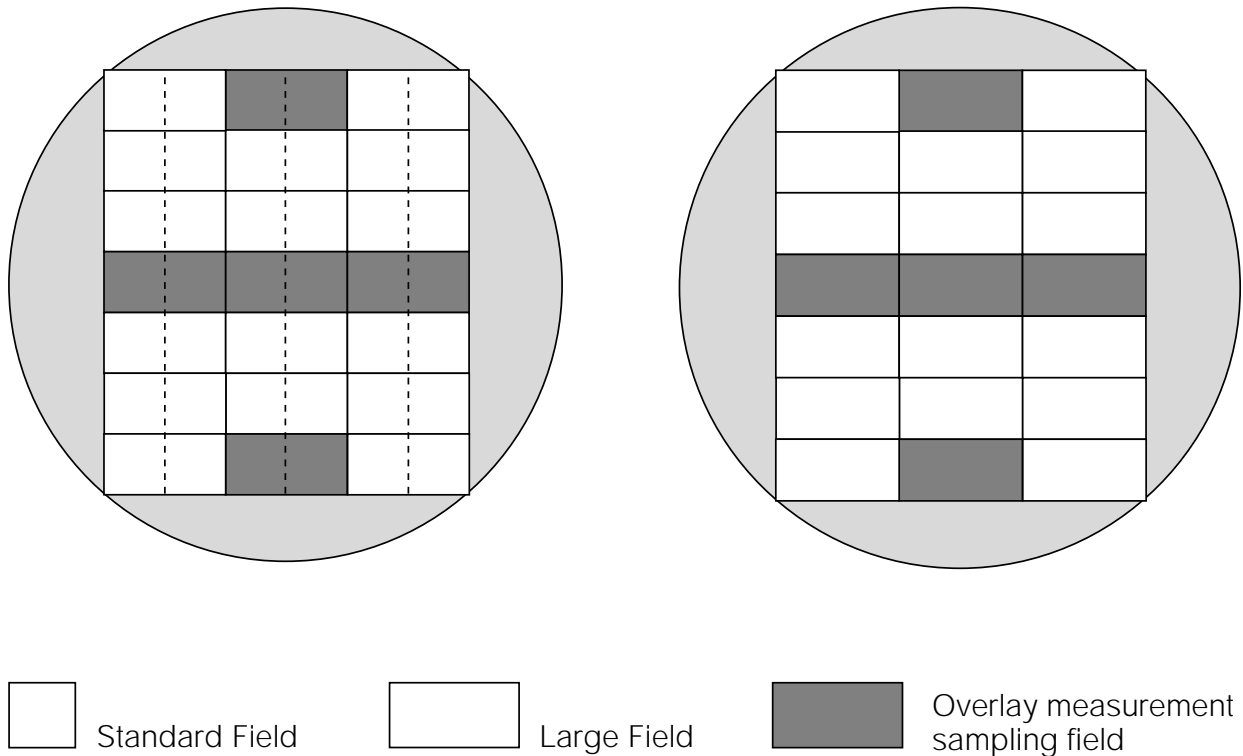


Figure 6: Wafer layout and sampling scheme for determining grid and intrafield model coefficients.

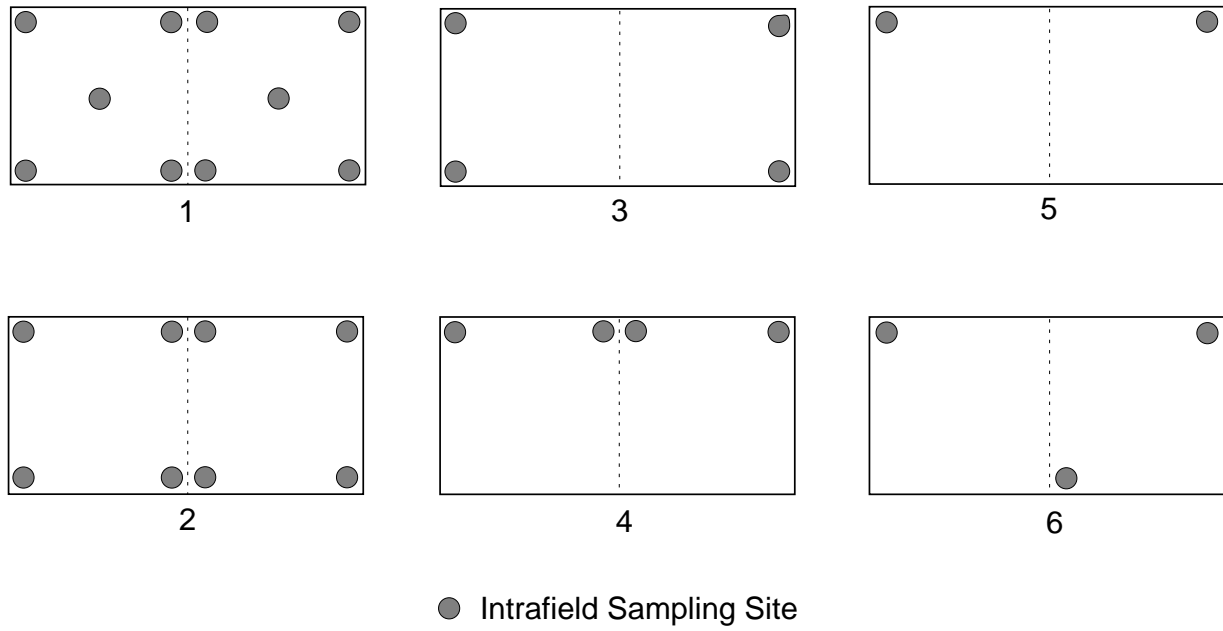


Figure 7: Intrafield sampling schemes used for determining grid and intrafield model coefficients.

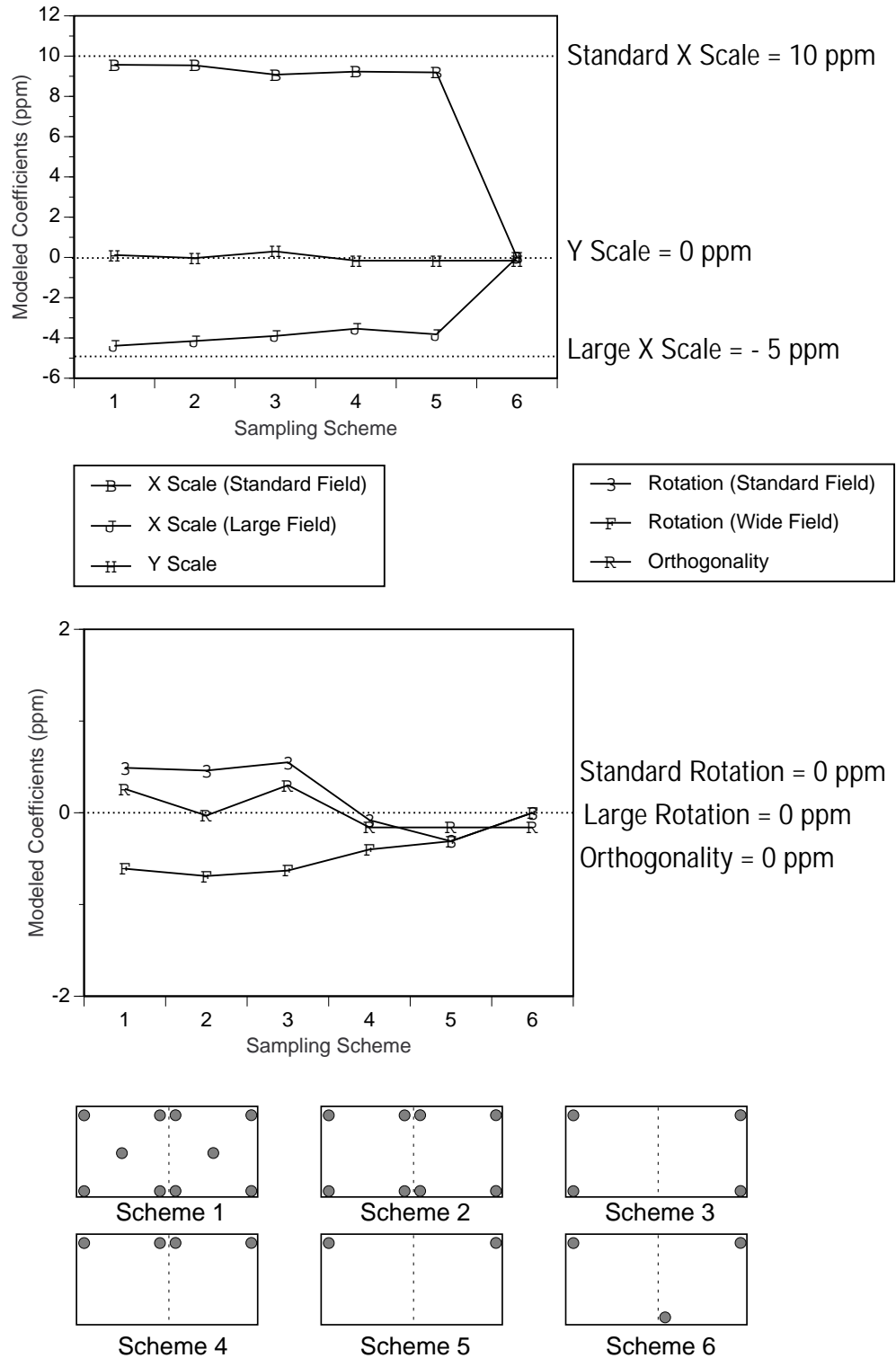


Figure 8: Modeled coefficients determined for X scale errors on the wafer grid. The standard field error is +10 ppm and the large field error is - 5 ppm.

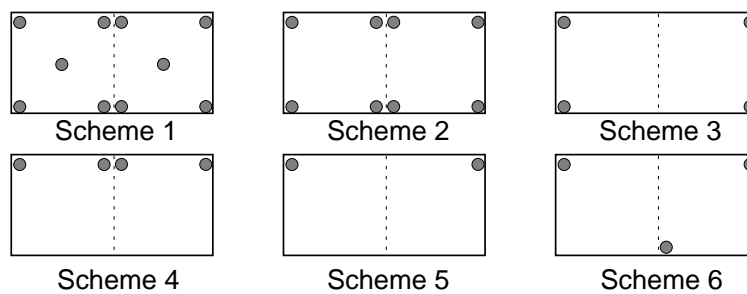
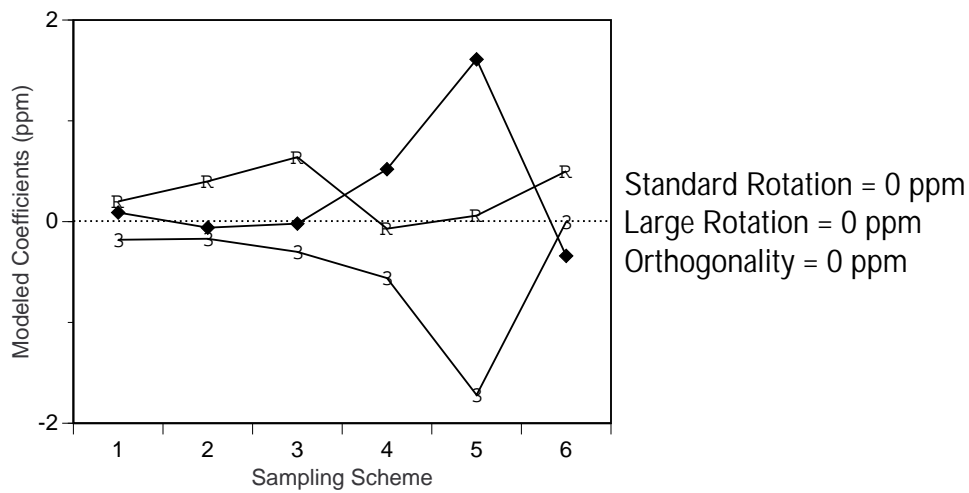
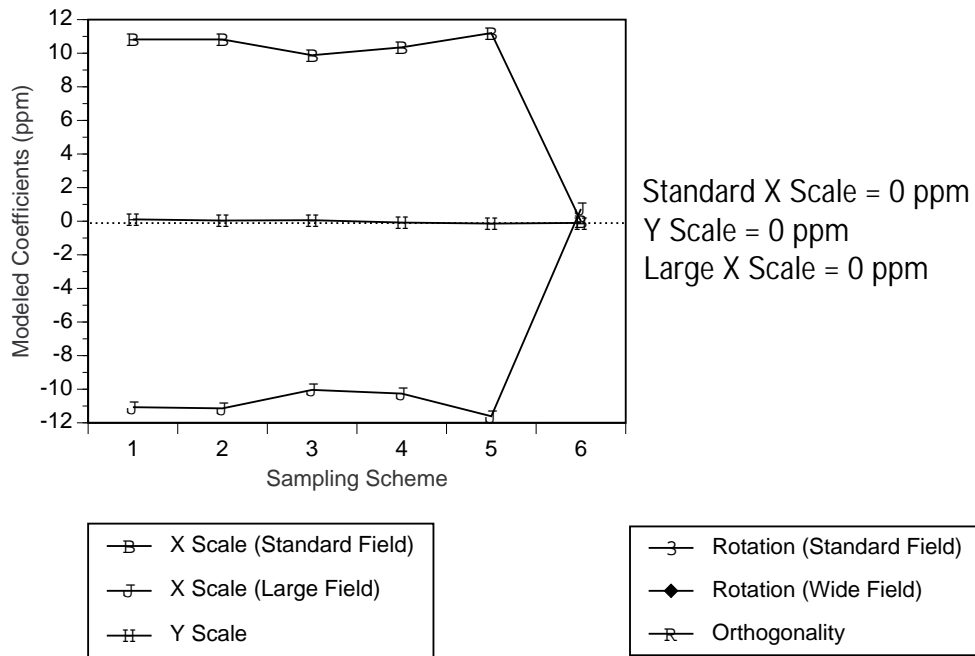


Figure 9: Modeled coefficients determined for intrafield magnification errors. The standard field error is 10 ppm and the large field error is -10 ppm.

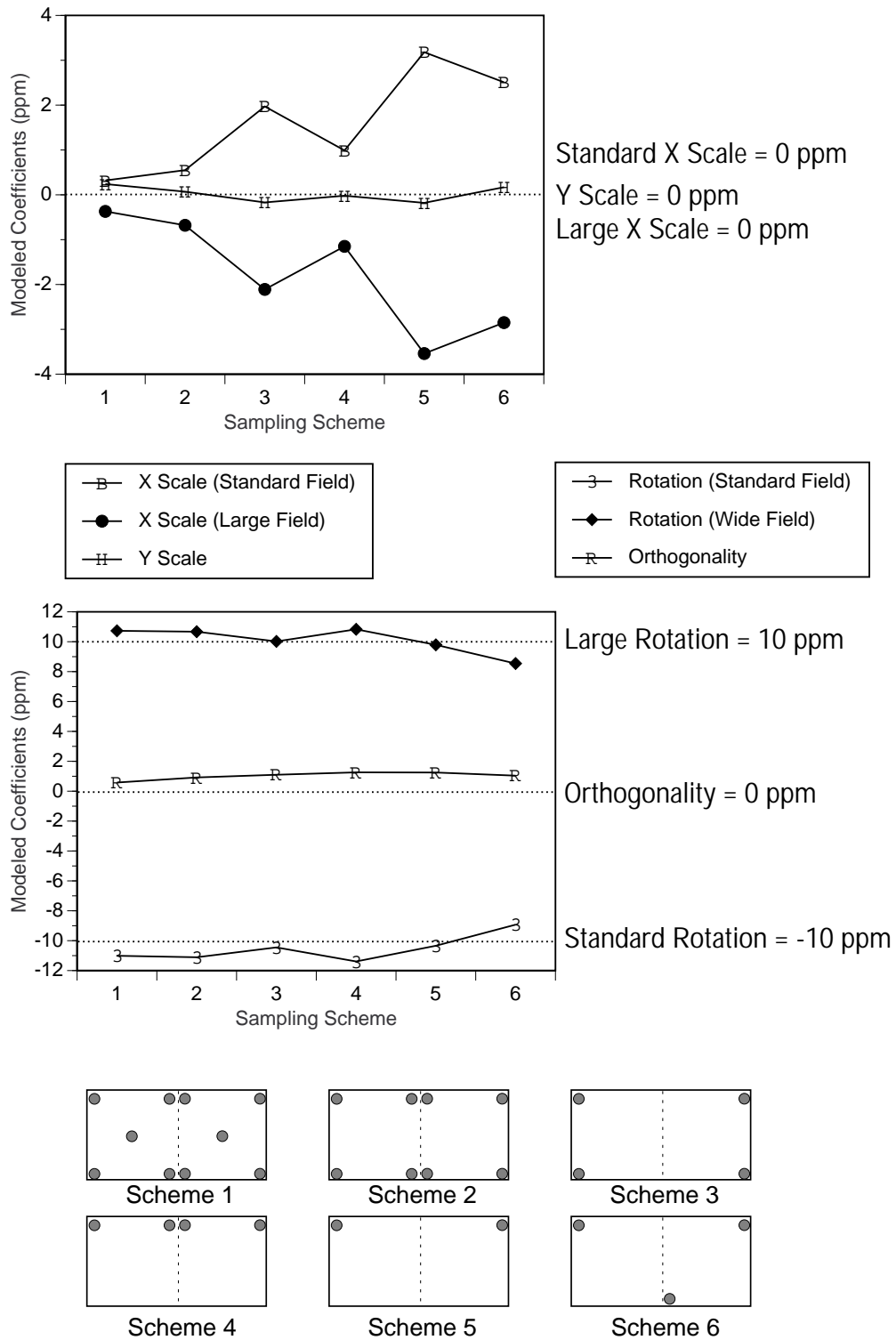


Figure 10: Modeled coefficients determined for orthogonality on the wafer grid. The standard field error is - 10 ppm and the large field error is + 10 ppm.

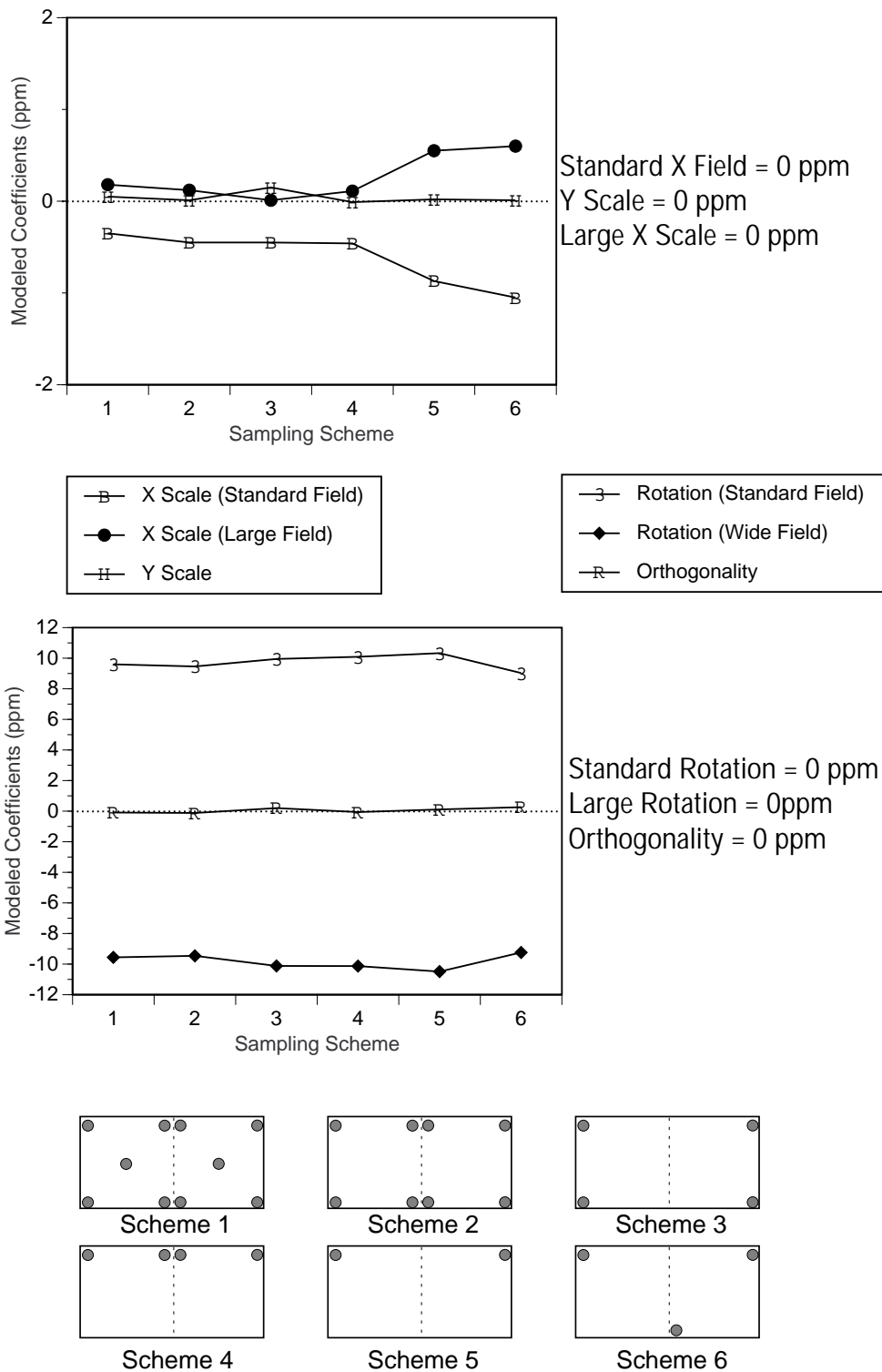


Figure 11: Modeled coefficients determined for intrafield rotation errors. The standard field error is -10 ppm and the large field error is + 10 ppm.

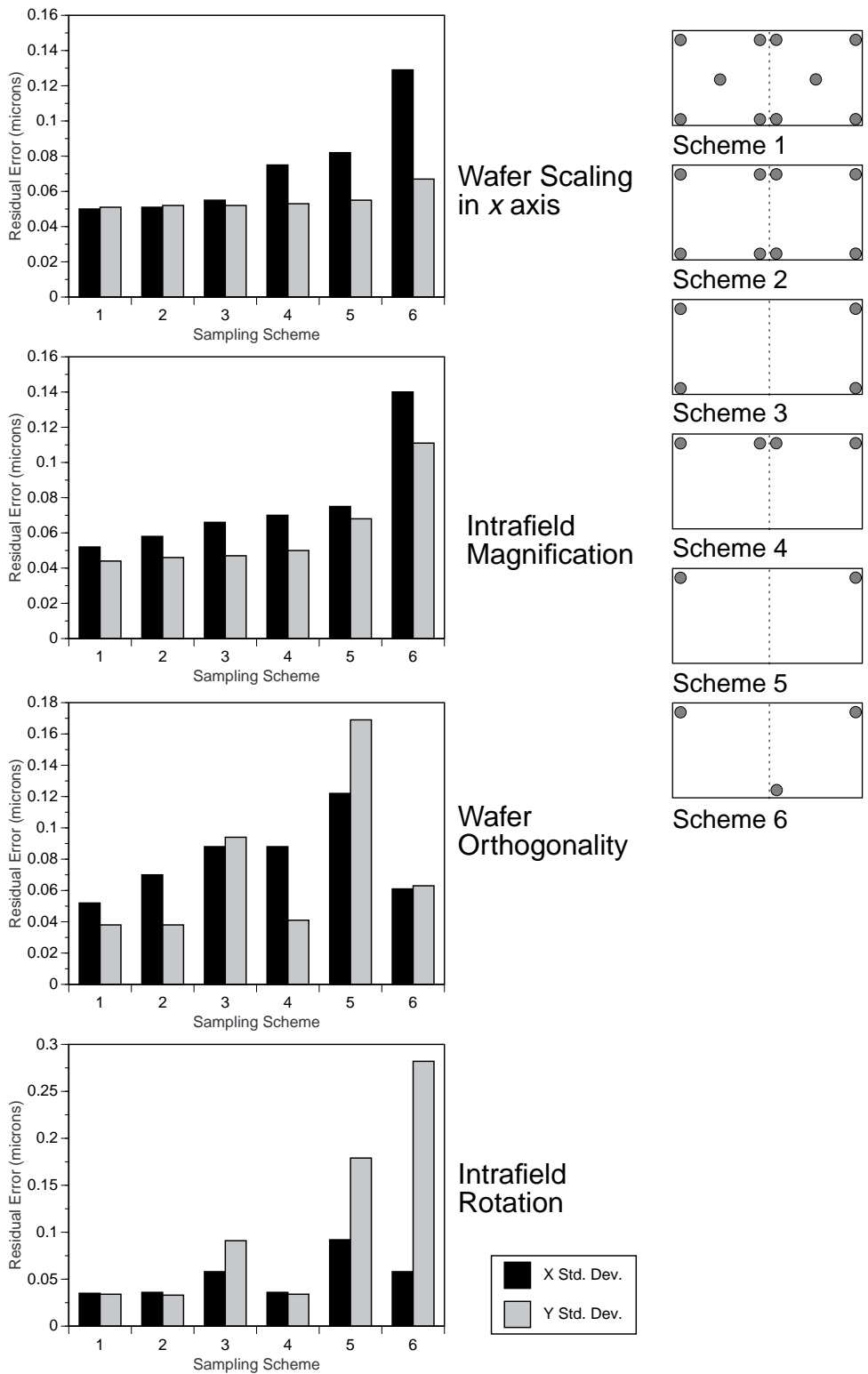


Figure 12: Residual x and y overlay errors for 2:1 registration as a function of sampling schemes. The examples are shown wafer scaling in x, intrafield magnification, wafer orthogonality and intrafield rotation.